

Regular paper

Photosystem II chlorophyll *a* fluorescence lifetimes and intensity are independent of the antenna size differences between barley wild-type and *chlorina* mutants: Photochemical quenching and xanthophyll cycle-dependent nonphotochemical quenching of fluorescence

Adam M. Gilmore^{1,*}, Theodore L. Hazlett², Peter G. Debrunner³ & Govindjee^{1,**}

¹Department of Plant Biology, University of Illinois at Urbana-Champaign, Urbana, IL 61801-3707 USA;

²Laboratory for Fluorescence Dynamics, University of Illinois at Urbana-Champaign, Urbana, IL 61801-3707

USA; ³Department of Physics, University of Illinois at Urbana-Champaign, Urbana, IL 61801-3707 USA;

*Present address: ANU/RSBS Photobioenergetics Group, Canberra, ACT0200, Australia; **Address for correspondence: Department of Plant Biology, UIUC, 265 Morrill Hall, 505 S. Goodwin Ave., Urbana, IL 61801-3707 USA

Received 4 December 1995; accepted in revised form 14 February 1996

Key words: antheraxanthin, chlorophyll *b* mutants, fluorescence lifetime distribution, *Hordeum vulgare* L., violaxanthin, zeaxanthin

Abstract

Photosystem II (PS II) chlorophyll (Chl) *a* fluorescence lifetimes were measured in thylakoids and leaves of barley wild-type and *chlorina* f104 and f2 mutants to determine the effects of the PS II Chl *a+b* antenna size on the deexcitation of absorbed light energy. These barley *chlorina* mutants have drastically reduced levels of PS II light-harvesting Chls and pigment-proteins when compared to wild-type plants. However, the mutant and wild-type PS II Chl *a* fluorescence lifetimes and intensity parameters were remarkably similar and thus independent of the PS II light-harvesting antenna size for both maximal (at minimum Chl fluorescence level, F_0) and minimal rates of PS II photochemistry (at maximum Chl fluorescence level, F_m). Further, the fluorescence lifetimes and intensity parameters, as affected by the trans-thylakoid membrane pH gradient (Δ pH) and the carotenoid pigments of the xanthophyll cycle, were also similar and independent of the antenna size differences. In the presence of a Δ pH, the xanthophyll cycle-dependent processes increased the fractional intensity of a Chl *a* fluorescence lifetime distribution centered around 0.4–0.5 ns, at the expense of a 1.6 ns lifetime distribution (see Gilmore et al. (1995) Proc Natl Acad Sci USA 92: 2273–2277). When the zeaxanthin and antheraxanthin concentrations were measured relative to the number of PS II reaction center units, the ratios of fluorescence quenching to [xanthophyll] were similar between the wild-type and *chlorina* f104. However, the *chlorina* f104, compared to the wild-type, required around 2.5 times higher concentrations of these xanthophylls relative to Chl *a+b* to obtain the same levels of xanthophyll cycle-dependent fluorescence quenching. We thus suggest that, at a constant Δ pH, the fraction of the short lifetime distribution is determined by the concentration and thus binding frequency of the xanthophylls in the PS II inner antenna. The Δ pH also affected both the widths and centers of the lifetime distributions independent of the xanthophyll cycle. We suggest that the combined effects of the xanthophyll cycle and Δ pH cause major conformational changes in the pigment-protein complexes of the PS II inner or core antennae that switch a normal PS II unit to an increased rate constant of heat dissipation. We discuss a model of the PS II photochemical apparatus where PS II photochemistry and xanthophyll cycle-dependent energy dissipation are independent of the Peripheral antenna size.

Abbreviations: Ax – antheraxanthin; BSA – bovine serum albumin; c_x – lifetime center of fluorescence decay component *x*; CP – chlorophyll binding protein of PS II inner antenna; DCMU – 3-(3,4-dichlorophenyl)-1,1-dimethylurea; DTT, dithiothreitol; f_x – fractional intensity of fluorescence lifetime component *x*; F_m , F_m' , maximal PS II Chl *a* fluorescence intensity with all Q_A reduced in the absence, presence of thylakoid membrane energization; F_0 – minimal PS II Chl *a* fluorescence intensity with all Q_A oxidized; $F_v = F_m - F_0$ – variable level of PS II Chl *a* fluorescence; HPLC – high performance liquid chromatography; k_A – rate constant of all combined energy

dissipation pathways in PS II except photochemistry and fluorescence; k_F – rate constant of PS II Chl *a* fluorescence; LHClIb – main light harvesting pigment-protein complex (of PS II); N_{pig} – mols Chl *a+b* per PS II; $NPQ = (F_m/F_m') - 1$ – nonphotochemical quenching of PS II Chl *a* fluorescence; PAM – pulse-amplitude modulation fluorometer; PFD, photon-flux density, $\mu\text{mols photons m}^{-2} \text{s}^{-1}$; PS II – Photosystem II; P680 – special-pair Chls of PS II reaction center; Q_A – primary quinone electron acceptor of PS II; V_x – violaxanthin; w_x – width at half maximum of Lorentzian fluorescence lifetime distribution x ; Zx – zeaxanthin; ΔpH – trans-thylakoid proton gradient; $\langle \tau \rangle_{F_0}$, $\langle \tau \rangle_{F_0} = \sum f_x c_x$ – average lifetime of Chl *a* fluorescence calculated from a multi-exponential model under F_m , F_0 conditions

Introduction

Photosynthetic light energy transduction begins when light energy is absorbed by the antenna chlorophylls (Chls) of the photosynthetic apparatus from which it is ultimately transferred to the photosynthetic reaction center. The classical experiments of Emerson and Arnold (1932a,b) laid the foundation for the concept of ‘the photosynthetic unit’ where only one in several hundred Chls functions as a photoenzyme while the rest serve an antenna function (Gaffron and Wohl 1936). The steps between light absorption by the antenna and charge separation and stabilization in the Photosystem II (PS II) reaction center, particularly the basic excitation energy transfer steps, have been discussed by several investigators (Pearlstein 1982; Dau 1994; van Grondelle et al. 1994). The prevailing theory regarding excitation energy transfer from the antenna to the reaction center holds that once light energy is absorbed, it is transferred as excitons rapidly (in steps on the order of a few hundred femtoseconds to a picosecond, Visser et al. (1995)) and more or less randomly among the many antennae Chls (Knox 1975; Pearlstein 1982). According to A. Holzwarth and coworkers (Holzwarth 1988; Schatz et al. 1988), all the PS II antenna Chls are in rapid excitonic equilibrium with the special Chls of the PS II reaction center, P680. The exciton radical pair equilibrium model (Schatz et al. 1988) as well as the tripartite model of Butler and Strasser (1977) assume that increasing the number (N_{pig}) of Chl *a+b* molecules in the photosystem decreases the probability of the exciton being trapped at P680 and increases the fluorescence lifetime of the exciton (see Dau 1994; van Grondelle et al. 1994). However, to our knowledge, the proposed relationship between N_{pig} and PS II fluorescence lifetimes has not been clearly demonstrated in higher plant leaves or thylakoids. Thus, our goal was to investigate the influence of N_{pig} on the PS II Chl *a* fluorescence lifetimes by using barley wild-type and *chlorina* f104 and f2 mutants that have different PS II antenna sizes (N_{pig}). Further, our study included

measurements of the fluorescence lifetimes not only at minimal (F_0) and maximal (F_m) Chl *a* fluorescence (and, thus, maximal and minimal rates of PS II photochemistry) but also during photoprotective xanthophyll cycle-dependent nonphotochemical quenching of fluorescence, NPQ, as described below.

Many recent studies have focused on the biochemical and biophysical aspects of the xanthophyll cycle-dependent mechanism that higher plants use to protect PS II under excess light conditions during environmental stress (for reviews, see Demmig-Adams et al. 1996; Yamamoto and Bassi 1996). The xanthophyll cycle-dependent photoprotection mechanism is suggested to dissipate excess excitation energy as heat in PS II (Horton et al. 1994; Gilmore et al. 1995a; Demmig-Adams et al. 1996). Since the three major decay pathways of the excited state are photochemistry (including energy transfer), fluorescence and heat, the increased heat loss decreases (quenches) the lifetimes and intensity yields of PS II Chl *a* fluorescence (Gilmore et al. 1995a,b). Although this mechanism is under complex influence of photosynthetic events at the thylakoid membrane level, it is primarily controlled by the trans-thylakoid pH gradient, ΔpH (Gilmore et al. 1995a). Acidification of the thylakoid lumen has two effects: first, the lumen pH activates the xanthophyll cycle deepoxidase enzyme (Hager 1969) which converts the diepoxide violaxanthin (V_x) to zeaxanthin (Zx) via the monooxide intermediate antheraxanthin (Ax) (Yamamoto et al. 1962) and second, the lumen pH protonates specific carboxyl residues on the minor light harvesting complexes of PS II, such as CP24, CP26 and CP29 (Crofts and Yerkes 1994; Horton et al. 1994; Walters et al. 1994). However, the role of protonation of other PS II complexes cannot as yet be excluded. Bassi et al. (1993) reported that the xanthophyll cycle pigments are mostly ($\approx 80\%$) concentrated in these minor CP proteins. It is further suggested that the protonation of the minor CP proteins leads to a special structural or binding interaction between the minor CP proteins and the xanthophylls that increases the rate constant of heat

dissipation in PS II (Horton et al. 1994; Gilmore et al. 1995a).

In this study, we have examined the PS II Chl *a* fluorescence lifetimes and intensity, as mentioned above, in barley wild-type and *chlorina* f104 and f2 mutants because they are well characterized regarding their widely different PS II Chl *a+b* antenna sizes (Simpson et al. 1985; Knoetzel and Simpson 1991; Harrison et al. 1993). These barley *chlorina* mutants are deficient in Chl *b* synthesis and accumulate drastically reduced levels of PS I and PS II antenna protein complexes including the major light-harvesting complex of PS II (LHCIIb). Growth at high light intensities exacerbates these deficiencies. In contrast to the decrease in the levels of mature Chl *b* containing antenna proteins, the levels of xanthophyll cycle pigments increase relative to the Chl *a+b* concentration (Knoetzel and Simpson 1991; Falbel et al. 1995). Despite the increased ratio of xanthophyll cycle pigments to Chl, the barley *chlorina* mutants exhibit similar (Falk et al. 1994b; Andrews et al. 1995) and in some cases significantly lower (Leverenz et al. 1992; Lokstein et al. 1994) levels of xanthophyll cycle-dependent fluorescence intensity quenching compared to the wild-type.

In this paper, we show from measurements of the PS II Chl *a* fluorescence lifetimes during xanthophyll cycle-dependent fluorescence quenching, by comparing *chlorina* f104 mutant and wild-type thylakoids, that the different PS II antenna sizes do not proportionally change the fluorescence lifetimes or intensity parameters. Although the lack of a relationship between the antenna size and fluorescence lifetimes, observed in this study, is inconsistent with earlier studies of the *chlorina* f2 mutant by Searle et al. (1979) and Karukstis and Sauer (1984), it is fully consistent with several other studies of the photosynthetic and fluorescence performance of the barley *chlorina* mutants (Leverenz et al. 1992; Briantais 1994; Falk et al. 1994a,b; Lokstein et al. 1994; Andrews et al. 1995). A preliminary account of our basic observations was presented at a conference (Gilmore et al. 1995b). We discuss here our results in terms of a hypothesis in which the peripheral PS II antenna size (mostly LHCIIb) does not affect the fluorescence lifetimes of PS II during photochemical de-excitation by the PS II reaction center or affect the level of xanthophyll cycle-dependent energy dissipation. Further, we present a 2-state PS II unit model to explain the ΔpH and xanthophyll cycle-dependent effects on the PS II Chl *a* fluorescence lifetimes.

Materials and methods

Plant material

Seeds of wild-type barley (*Hordeum vulgare* L. cv. Donaria) and the nuclear gene mutants *chlorina* f2 and *chlorina* f104 were obtained from Dr D. Simpson of the Carlsberg Research laboratories, Copenhagen Valby, Denmark. For high-light growing conditions, seeds were germinated in a glasshouse in potting soil covered with a light layer of vermiculite and on a heating pad for three days. In addition to ambient sunlight conditions, the glasshouse benches were fitted with supplemental high intensity lamps such that the photon flux density (PFD) at the bench top level was at least $400 \pm 100 \mu\text{mol m}^{-2} \text{s}^{-1}$ and the photoperiod was 14 h. Plants were watered twice daily and fertilized once with a 20 N:20 P:20 K fertilizer applied at a concentration of 473 ppm N.

For comparison of the effects of varying PFDs on the ratio of Chl *a*/Chl *b* and the PS II Chl *a+b* antenna size, barley wild-type and *chlorina* f104 seeds were grown in a growth chamber (Conviron model CMP 3023) at three PFDs: 310 ± 23 , 236 ± 17 and $143 \pm 13 \mu\text{mol m}^{-2} \text{s}^{-1}$. The photoperiod (and temperature) was 14 h light (22 °C) and 10 h dark (20 °C). Plants were watered daily with a dilute mixture (0.25 teaspoons to 1 gallon of water) of Miracle-Gro® (15 N: 30 P: 15 K).

Measurements of PS II Chl *a* fluorescence lifetimes

Fluorescence lifetimes were measured with a multifrequency cross-correlation fluorimeter (Model K2, ISS Instruments, Urbana, IL). The average PFD of the sinusoidally modulated sample excitation was $24 \pm 4 \mu\text{mol m}^{-2} \text{s}^{-1}$ at 610 nm (for measurements on thylakoids) or 595 nm (for measurements on leaves) and was provided by a cavity-dumped rhodamine 6G dye laser pumped by a mode-locked Nd-YAG laser (Coherent, Palo Alto, CA). Data were collected at sixteen separate frequencies of the sinusoidally modulated excitation ranging from 7 to 300 MHz. The frequencies were mixed randomly during acquisition to minimize systematic errors from sample bleaching and heterogeneity. The sample emission was collected with the emission monochromator polarizer set at the 'magic-angle' (54.7°) and filtered through a Hoya R-68 red filter. The shift in phase angles and demodulation ratios of the sample fluorescence emission were recorded and analyzed as described below. Light scattering from a

glycogen suspension was used for the lifetime = 0 ns reference. Further details and explanation of the multifrequency cross-correlation technique including the equations used to describe the phase shift and demodulation ratio can be found in Govindjee et al. (1993).

*Thylakoid sample preparation and measurements of xanthophyll cycle-dependent quenching of PS II Chl *a* fluorescence*

For thylakoid isolation, leaves were harvested from the high-light glasshouse grown 7- to 14-day-old plants after at least 12 hours of dark adaptation at room temperature. Leaves were then chilled to 4 °C for 1 to 2 hours prior to thylakoid isolation as described by Gilmore and Yamamoto (1993). In the water jacketed reaction cuvette (15 °C), the thylakoid suspension was osmotically shocked for 15 s by a 1:10 dilution in 5 mM MgCl₂. The thylakoid reaction medium was brought to a final volume of 5 ml and a Chl *a+b* concentration of 15 μM and contained 30 mM Na-ascorbate, 50 μM methylviologen, 0.3 mM ATP, 0.1 M sucrose, 10 mM NaCl, 10 mM KCl, 5 mM MgCl₂, 10 mM Tricine, 1 mM KH₂PO₄, 0.2% BSA, pH 8.0.

We emphasize that we measured, in parallel to the fluorescence lifetime measurements, changes in the PS II Chl *a* fluorescence intensity with the pulse amplitude modulation fluorometer (PAM 103, Heinz-Walz, Effeltrich, Germany). The PS II Chl *a* fluorescence intensity in the presence of maximal PS II photochemistry, F_v , was measured from the top surface of the reaction cuvette with a $<0.15 \mu\text{mol photons m}^{-2}\text{s}^{-1}$ (1.6 kHz) beam, and the maximal fluorescence intensity in the presence of minimal PS II photochemistry, F_m , was measured with a 100 kHz PAM measuring beam during a 2 s light pulse ($5000 \mu\text{mol photons m}^{-2}\text{s}^{-1}$ after passing through a Walz DT-Cyan filter).

Xanthophyll cycle-dependent nonphotochemical quenching was induced by a white continuous actinic light ($500 \mu\text{mol photons m}^{-2}\text{s}^{-1}$, Corning CS1-75 infrared filter) turned on while the PAM measuring beam was switched to 100 kHz. The [Zx+Ax] (concentrations are listed within square brackets in this paper) was controlled by the dithiothreitol (DTT) concentration added before illumination, i.e., 3 mM for complete inhibition and usually <0.25 mM for subsaturating inhibition (Gilmore and Yamamoto 1993). After 15 min light exposure, 3 mM dithiothreitol was added to stop deepoxidation (Yamamoto and Kamite 1972) and to assure thiol-activation of the ATPase (Petrack and Lipman 1961; Mills and Mitchell 1982).

A 1.5 ml aliquot from each light-treated sample (15 μM Chl *a+b*) was treated with 2 μM nigericin and saved at -80 °C for HPLC pigment analysis (Gilmore and Yamamoto 1991). A portion of the sample was then diluted to a final volume of 3 ml and 7.5 μM Chl *a+b* for the fluorescence lifetime measurements; all other reagents were the same as in the reaction mixture above except DCMU (10 μM) was added to inhibit Q_A⁻ oxidation. The quenched sample was analyzed in the lifetime instrument at 2 °C within ≈15 min; the 2 °C sample temperature was used to help stabilize the ATPase mediated ΔpH and, thus, the level of NPQ during the data acquisition, see Gilmore and Björkman (1995). Under these conditions, the ATPase mediated ΔpH and NPQ remained at steady state for >0.5 h. After the fluorescence lifetime measurements, the sample was immediately placed under the PAM where the quenched F'_m was measured with a 100kHz PAM measuring beam in the presence of a white actinic PFD = $500 \mu\text{mol m}^{-2}\text{s}^{-1}$; after the ΔpH was uncoupled with nigericin (2 μM) the unquenched F_m was determined. The unquenched fluorescence lifetime data were either immediately taken or the samples stored (dark 0 °C) until the measurements on the quenched samples were finished; neither the fluorescence lifetimes nor F_m changed during ice storage (<3 h).

The steady state PS II Chl *a* fluorescence intensity parameters (F_m , F'_m , and F_o) used in this study were as described by van Kooten and Snel (1990). The ratio of the variable fluorescence ($F_v = F_m - F_o$) to the maximal fluorescence yield F_m , F_v/F_m , was measured as an indicator of the quantum yield of PS II (Björkman and Demmig 1987; see Govindjee 1995 for a review). The decrease in the PS II Chl *a* fluorescence intensity due to the xanthophyll cycle-dependent effect was defined as nonphotochemical quenching, NPQ = $(F_m/F'_m) - 1$.

*Leaf sample preparations and PS II Chl *a* fluorescence measurements*

Before measurements of the fluorescence intensity and lifetimes, barley plants (7 to 14 days old) were dark adapted for at least 1 hour. Fluorescence intensity yields were determined for secondary or primary leaves by first measuring the minimal fluorescence intensity (F_o) with a weak, 1.6 kHz PAM measuring beam (PFD $<0.2 \mu\text{mol m}^{-2}\text{s}^{-1}$). The maximal fluorescence intensity (F_m) was then determined by applying one strong 3 s pulse of white light (PFD $>10,000 \mu\text{mol m}^{-2}\text{s}^{-1}$)

while simultaneously switching the PAM measuring beam to 100 kHz (PFD $\approx 5 \mu\text{mol m}^{-2} \text{s}^{-1}$).

For the fluorescence lifetime determinations under F_m and F_o conditions, pieces (2–3 cm) of primary or secondary leaves were first vacuum infiltrated with either 10 μM DCMU or water, respectively, then incubated in it in the dark for 30 min at normal atmosphere and room temperature. The adaxial surfaces of the leaf pieces were gently packed with cotton flat against the front surface inside a triangular fluorescence cuvette and the cuvette was filled with either water or 10 μM DCMU solution. The average PFD of the sinusoidally modulated 595 nm exciting beam of the fluorescence lifetime instrument defined above was either $26 \pm 2 \mu\text{mol m}^{-2} \text{s}^{-1}$ for measuring the average lifetime under F_m conditions, $\langle \tau \rangle_{F_m}$, or $0.20 \pm 0.05 \mu\text{mol m}^{-2} \text{s}^{-1}$ for measuring $\langle \tau \rangle_{F_o}$ under F_o conditions (see Figure 4 under 'Results' for details of calculation of $\langle \tau \rangle_{F_m}$ and $\langle \tau \rangle_{F_o}$). As for the thylakoid samples, the PS II Chl *a* fluorescence emission was monitored at sixteen frequencies between 7 and 300 MHz. All other fluorescence lifetime acquisition parameters as well as the glycogen light scatterer (lifetime = 0 ns) reference were the same as above for the thylakoid preparations. The leaf sample fluorescence lifetime measurements were completed within 1.5 hours after cutting from the plant.

The Chl *a*/Chl *b* ratios were determined from each sample by grinding the (2–3 cm long) leaf pieces in 5 ml of 80% acetone in a chilled tissue-grinder (in an ice-bucket) until the remaining tissue was visibly white and free of Chl. The solution was brought to a final 85% acetone, vortexed for 30 s then clarified by micro-centrifugation. Absorbance at 663.6 nm and 646.6 nm were determined in a dual-beam spectrophotometer (Shimadzu model UV 160 U). The Chl *a*/Chl *b* ratios were calculated according to the equations used in Graan and Ort (1984); similar results (within 5%, not shown) were obtained using the method of Porra et al. (1989)

Analysis of multifrequency cross-correlation phase and modulation data

The acquired multifrequency phase and modulation data were fit to either a bimodal Lorentzian distribution model or a multi-component discrete exponential model using Globals Unlimited software (Laboratory for Fluorescence Dynamics, Physics Department, University of Illinois at Urbana-Champaign, Urbana, IL). The fluorescence lifetime data were presented

as the lifetime centers (c_x) and fractional intensities ($f_x = \alpha_x c_x / \sum \alpha_x c_x$, where α_x is the pre-exponential amplitude factor representing the fractional contribution of the component x with the fluorescence lifetime center c_x). The data sets could not be fit with more than the reported number of Lorentzian distributions or discrete exponential components; inclusion of another lifetime component either resulted in a duplicate lifetime value and/or in components with physically suspect values. Addition of another component did not significantly improve the χ^2 minimum.

We found, when considering the ΔpH and xanthophyll cycle effects, that the bimodal Lorentzian distribution model yielded, on average (see bottom of Table 1), slightly better χ^2 fits for the multifrequency phase and modulation data than a three component exponential decay model for the same thylakoid samples and conditions. However, the patterns of change in the fractional intensities and lifetime values, to be described below, for the Lorentzian distribution model were very similar to the changes in the two major lifetime component parameters from the three component exponential decay model; thus, the exponential data are not shown. Our analysis of the time-resolved data using a continuous Lorentzian distribution of lifetimes considers the following physical assumptions: The Chl fluorescence lifetime is strongly influenced by its molecular surroundings; the various pigment protein complexes, that contain (bind) Chl, exist in a distribution of multiple conformational substates or shapes (Frauenfelder et al. 1988); and, the different conformational substates may interconvert within the time frame of the Chl fluorescence lifetime (Govindjee et al. 1993).

Results

PS II Chl a Lorentzian fluorescence lifetime distributions during xanthophyll cycle-dependent quenching in barley wild-type and chlorina f104 thylakoids

Figure 1 illustrates the PS II Chl *a* fluorescence distributions in the same barley wild-type thylakoid samples under (A) conditions without an ATPase mediated ΔpH (for unquenched fluorescence) and (B) in the presence of an ATPase mediated ΔpH (for quenched fluorescence). In both (A) and (B) the $[Zx+Ax]$ varied from sample to sample ($n = 19$) by up to a factor of 5 or 6. Both the major (2 ns) and minor (0.1 ns) lifetime distributions in panel A were remarkably invariant for

Table 1. Effects of the absence (unquenched) and presence (quenched) of a trans-thylakoid pH gradient, ΔpH , on the Mean \pm SE bimodal Lorentzian PS II Chl *a* fluorescence lifetime distribution center, width, fractional intensity and χ^2 parameters for barley wild-type and *chlorina* f104 thylakoids. Also listed are the χ^2 fits for a three component exponential decay model for the same thylakoid samples and conditions

Parameter ^a	WT (<i>n</i> = 19)		f104 (<i>n</i> = 13)	
	Unquenched	Quenched	Unquenched	Quenched
c_1 (ns)	1.94 \pm 0.02	1.61 \pm 0.02	1.90 \pm 0.02	1.67 \pm 0.03
c_2 (ns)	0.19 \pm 0.01	0.40 \pm 0.03	0.01 \pm 0.00	0.52 \pm 0.04
w_1 (ns)	0.76 \pm 0.01	0.30 \pm 0.02	1.07 \pm 0.02	0.76 \pm 0.06
w_2 (ns)	0.18 \pm 0.03	1.06 \pm 0.06	1.42 \pm 0.04	0.90 \pm 0.10
f_1	0.93 \pm 0.00	Variable ^b	0.90 \pm 0.01	Variable
f_2	0.07 \pm 0.00	Variable	0.15 \pm 0.03	Variable
χ^2 (Lorentzian)	1.53 \pm 0.32	2.36 \pm 0.21	1.06 \pm 0.10	3.98 \pm 0.44
χ^2 (Exponential)	1.67 \pm 0.29	2.42 \pm 0.20	1.82 \pm 0.20	4.53 \pm 0.41

^a All lifetime center (c_x) and width (w_x) values in the Table were constant and did not significantly correlate with either the level of NPQ or the [Zx+Ax].

^b The values listed as variable correlated significantly with both NPQ and the [Zx+Ax].

all the samples without a ΔpH . The arrow heads in Figure 1B show the direction of the effects of increasing concentrations of Zx+Ax in the presence of a ΔpH on the fractional intensities of the two fluorescence lifetime distributions, c_1 (longer lifetime component) and c_2 (shorter lifetime component). The major observation is that the fractional intensity of c_2 increases at the expense of the fraction of c_1 with increasing NPQ, confirming Gilmore et al. (1995a). Similar data (not shown) were obtained for the *chlorina* f104 thylakoids in agreement with our preliminary report (Gilmore et al. 1995b)

In Table 1 we quantitatively compare the effects of xanthophyll cycle-dependent PS II Chl *a* fluorescence quenching on the bimodal Lorentzian distribution fluorescence lifetime center, width and fractional intensity parameters obtained with wild-type and *chlorina* f104 thylakoids. As is evident from Figure 1A for unquenched WT thylakoids, the fluorescence lifetime centers (c_1 and c_2), widths (w_1 and w_2) and fractional intensity parameters (f_1 and f_2) have small standard errors and thus vary little from sample to sample for each thylakoid type without a ΔpH . The main ($\geq 90\%$) distribution, c_1 , was around 1.9 ns with a width of 0.75 and 1.1 ns for the wild-type and f104 thylakoids, respectively. The minor ($\approx 10\%$) c_2 distribution had a lifetime center less than 200 ps in both types of thy-

lakoids; however, w_2 was significantly wider in the f104 than in the wild-type.

Under the quenched conditions (with a ΔpH) both the fluorescence lifetime center values (c_1 and c_2) and width parameters (w_1 and w_2) switch to significantly different values from those under unquenched conditions for both the wild-type and f104 mutant. Three prominent changes distinguished the state of the quenched (+ ΔpH) from the unquenched ($-\Delta\text{pH}$) PS II Chl *a* fluorescence, namely: 1) the lifetime center (c_1) became about 200 to 300 ps shorter, 2) the width (w_1) became around 300 ps narrower and 3) the lifetime center (c_2) became longer under the quenched compared to unquenched conditions in each thylakoid type. Importantly, although the lifetime centers (c_1 and c_2) and widths (w_1 and w_2) switched to new values under the quenched conditions, the standard errors remained small for both types of thylakoids. On the average, w_1 was slightly wider in the f104 mutant than in the WT under both quenched and unquenched conditions, as was w_2 under the unquenched conditions. On the other hand, the c_2 and w_2 values under the quenched conditions were similar for both types of thylakoids. We suggest that the quenched state (described by c_2 , f_2 , w_2) represents a similar conformational state in both thylakoid types probably owing to the effects of the ΔpH and xanthophylls.

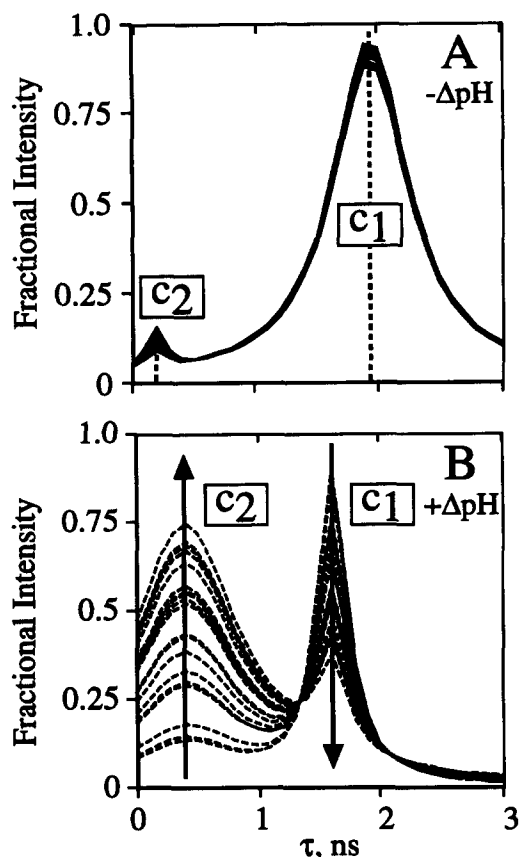


Figure 1. Effects of xanthophyll cycle-dependent nonphotochemical quenching (NPQ) on the PS II Chl *a* fluorescence lifetime distributions in barley wild-type thylakoids. Panel A shows the bimodal Lorentzian distributions of 19 samples without a trans-thylakoid Δ pH (under the unquenched conditions for the fluorescence). Panel B shows the lifetime distributions for the same 19 samples as in Panel A with a trans-thylakoid Δ pH (under quenched conditions for the fluorescence). The curves were drawn using the average width and lifetime center values and the actual fractional intensity values for either the conditions without a Δ pH (A) or with a Δ pH (B); the standard error values are given Table 1. The directions of the arrows in Panel B represent the effects of increasing concentrations of Zx+Ax and xanthophyll cycle-dependent NPQ under the quenched conditions. The unquenched (3 ml) thylakoid reaction mixture in Panel A contained 7.5 μ M Chl *a+b*, variable levels of [Zx+Ax], 10 μ M DCMU, 2 μ M nigericin, 30 mM Na-ascorbate, 50 μ M methylviologen, 0.3 mM ATP, 0.1 M sucrose, 10 mM NaCl, 10 mM KCl, 5 mM MgCl₂, 10 mM Tricine, 1 mM KH₂PO₄, 0.2% BSA, pH 8.0. The quenched sample reaction mixture in Panel B was the same as in A except without nigericin.

The average χ^2 values of the fits in Table 1 were similar for both types of thylakoids under the unquenched conditions. Under the quenched conditions, there was a slight but significant increase in the χ^2 value for both the wild-type and f104 thylakoids attributed to the relative instability or heterogeneity of

the quenched compared to unquenched state; the residuals (not shown) indicated that this noise was randomly distributed around the mean and not systematic with respect to frequency.

Figure 2 shows the correlation between the Lorentzian fractional intensity parameter f_2 and the decrease in the PS II Chl *a* fluorescence intensity measured both as NPQ = $(F_m/F_m') - 1$ (Panel A) and as the F_m' intensity (relative to F_m) (Panel B) for the barley wild-type (circles) and *chlorina* f104 thylakoids (squares). Over the observed range of NPQ (0–0.7) measured in the presence of the ATPase mediated Δ pH we observed a large (up to 75%) conversion to the f_2 distribution. As shown in the inset in Figure 2, the relationship between f_2 and NPQ is approximately linear over the experimentally observed range, being quite similar for both thylakoid types despite their different Chl *a*/Chl *b* ratios and PS II Chl *a+b* antenna sizes, see Figure legend. However, as shown by the curves in Figure 2A, our arguments predict that further increases in f_2 beyond those experimentally measured in the presence of the ATPase mediated Δ pH should result in an increasingly steep relationship between f_2 and NPQ. Based on our bimodal distribution model, plotting NPQ = $(F_m/F_m') - 1$ against F_m' , which is an increasing function that has a nearly linear portion over the range of NPQ values below 1. Indeed, it is clear in Figure 2B that F_m' and the f_2 component are linearly related in a similar manner in both the WT and f104. The bars along the top of Figure 2A and lower region of Figure 2B represent the Mean \pm SD maximal levels of NPQ and minimal levels of F_m' , respectively, measured with the PAM fluorometer in the wild-type (hatched bar, dashed line) and *chlorina* f104 (open bar, solid line) thylakoids during the light-induction portion of the experimental protocol; the conditions included the presence of a light-induced Δ pH and high-levels of [Zx+Ax], see Figure legend. The maximal levels of NPQ and minimal levels of F_m' in the light, like the maximal levels in the presence of the ATPase mediated Δ pH (symbols), were virtually identical for the wild-type and *chlorina* f104 samples. Importantly, based on the predicted relationships between f_2 and NPQ and F_m' , extrapolation from the maximal levels of NPQ obtained with the ATPase mediated Δ pH (symbols) to the maximal levels in the light would only require a slight (< 20%) increase in the fractional intensity of the f_2 component. This is not surprising because the differences in the F_m' intensity between a value of NPQ = 0.7 to NPQ = 1.5 are also less than 20% of F_m (Fig-

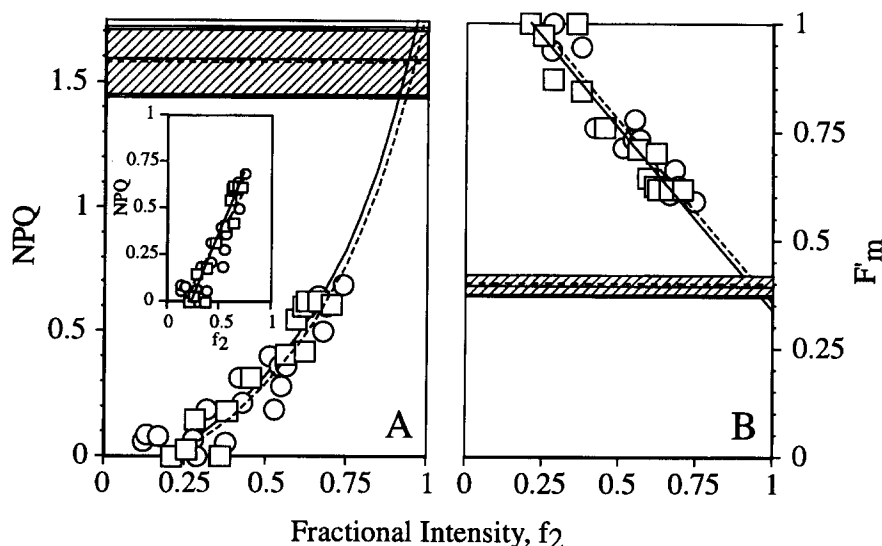


Figure 2. Relationships between the Lorentzian fractional intensity parameter, f_2 , and xanthophyll cycle-dependent nonphotochemical quenching ($NPQ = (F_m/F_m') - 1$) of the maximal yield of PS II Chl *a* fluorescence (F_m') in barley wild-type (circles, dashed line) and *chlorina* f104 thylakoids (squares, solid line). The predicted curves in (A) were calculated by substituting values for f_2 with the calculated values for F_m' based on the linear relationship between f_2 and F_m' shown in panel B. The inset Figure (A) shows the same data fit to a simple linear regression; the correlation coefficients for the fits were $r^2 = 0.80$ and $r^2 = 0.91$ for the wild-type and *chlorina* f104, respectively. The linear equations describing the fits in (B) were $F_m' = -0.84(f_2) + 1.18$; $r^2 = 0.90$ for the *chlorina* f104 and $F_m' = -0.84(f_2) + 1.19$; $r^2 = 0.90$ and wild-type. The bars in Figure 2A and 2B, respectively, represent the Mean \pm SD maximal levels of NPQ and minimal levels of F_m' measured in the barley wild-type (hatched bar, dashed line) and *chlorina* f104 (open bar, solid line) thylakoids containing the highest levels of [Zx+Ax] during the light-induction portion of the experimental protocol described in the 'Materials and method'; the wild-type thylakoid samples ($n = 4$) contained 32 ± 2 and the *chlorina* f104 ($n = 5$) thylakoids contained $75 \pm 9 \mu\text{mol Zx+Ax (mol Chl } a+b)^{-1}$. The Chl *a*/Chl *b* ratios (and estimated N_{pig} values) were 6.05 ± 0.15 (133) and 3.59 ± 0.05 (250) for the *chlorina* f104 and wild-type, respectively; N_{pig} calculations were based on the data presented by Knoetzel and Simpson (1991).

ure 2B). Further, our extrapolations suggest that near 100% conversion to the f_2 component is possible under conditions of a light-induced ΔpH and high [Zx+Ax].

Comparison of xanthophyll cycle pigment stoichiometry to the Lorentzian distribution fractional intensities and nonphotochemical quenching of PS II Chl a fluorescence in the wild-type and chlorina f104 thylakoids

Figure 3 shows the relationship between the [Zx+Ax] and both the NPQ and the fractional intensity of the short-lived Lorentzian f_2 component in the presence of the ATPase mediated ΔpH from wild-type (circles) and *chlorina* f104 (squares) thylakoids. Table 2 shows the linear regression statistics for the data fits in Figure 3. There was a significant linear correlation between the [Zx+Ax] and both NPQ and also f_2 over this experimentally observed range. Importantly, the maximal percentage of Vx deepoxidation in relation to NPQ was similar, being slightly higher for the f104 thylakoids ($[\text{Zx+Ax}]/[\text{Zx+Ax+Vx}] \approx 60\%$) com-

pared to the WT ($\approx 50\%$) (see Figure 3 legend for the $[\text{Vx+Zx+Ax}] : [\text{Chl } a+b]$). However, Figures 3A and C show that when expressed relative to Chl *a+b*, almost 2.5 times as much Zx+Ax was needed to obtain the same f_2 or NPQ in the f104 than in the WT thylakoids under the ATPase mediated ΔpH conditions. When relating the level of NPQ to the [Zx+Ax], it was necessary, as shown by Gilmore et al. (1993), to consider the number of mols of Ax with equal weight to Zx to obtain both the satisfactory correlation coefficients (r^2) and the significant ($P \leq 0.05$) negative intercept values in Table 2. Interestingly, if we assume an equal and constant ΔpH in both the *chlorina* f104 and WT samples [as would be expected from ATP hydrolysis under these conditions (Gilmore and Yamamoto 1992; Gilmore et al. 1995a)], then it is clear that the level of NPQ in each thylakoid type is not similarly determined by the ratio of $[\text{Zx+Ax}] : [\text{Chl } a+b]$. However, when expressed relative to the estimated number of PS II reaction centers (based on the estimated molar PS II antenna size = N_{pig} , see Figure 2 legend and Table 2) the slopes in Figures 3B and D for the *chlori-*

Table 2. Linear regression statistics^a for the relationships between nonphotochemical quenching (NPQ) and the ^bfractional intensity parameter (f_2) and the concentration of Zx+Ax in both barley wild-type (WT, $n = 19$) and *chlorina* f104 (f104, $n = 13$) mutant thylakoids. The Zx+Ax concentration was expressed relative to both Chl *a+b* and the ^cestimated number of PS II reaction centers

Model equation: NPQ or $f_2 = \text{Slope} [(\mu\text{mol Zx + Ax})/(\text{mol Chl } a+b)] + \text{Intercept}$			
	Slope; (<i>P</i>)	Intercept; (<i>P</i>)	r^2
NPQ WT	$(20.88 \pm 1.61) \times 10^{-3}$; (1.37×10^{-10})	-0.07 ± 0.03 ; (3.8×10^{-2})	0.91 ± 0.07
NPQ f104	$(8.75 \pm 0.74) \times 10^{-3}$; (5.8×10^{-8})	-0.11 ± 0.04 ; (2.5×10^{-2})	0.93 ± 0.07
f_2 WT	$(17.40 \pm 1.97) \times 10^{-3}$; (5.8×10^{-8})	0.14 ± 0.04 ; (2.3×10^{-3})	0.82 ± 0.08
f_2 f104	$(5.93 \pm 0.60) \times 10^{-3}$; (4.27×10^{-7})	0.18 ± 0.04 ; (2.9×10^{-4})	0.90 ± 0.06

Model equation: NPQ or $f_2 = \text{slope} [(\text{mol Zx + Ax})/(\text{mol PS II RC})] + \text{intercept}$			
	Slope	Intercept	r^2
NPQ WT	8.35 ± 0.01	-0.07 ± 0.03	0.91 ± 0.07
NPQ f104	6.60 ± 0.01	-0.11 ± 0.04	0.93 ± 0.07
f_2 WT	6.96 ± 0.01	0.14 ± 0.04	0.82 ± 0.08
f_2 f104	4.47 ± 0.00	0.18 ± 0.03	0.90 ± 0.06

^a r^2 , coefficient of determination; *P*, probability for null hypothesis of the slope or intercept parameter

^bThe linear regression fits are only assumed to apply to the limited experimental range for the f_2 parameter

^cThe estimated N_{pig} values were 250 for the WT and 133 for the *chlorina* f104, see Knoetzel and Simpson (1991)

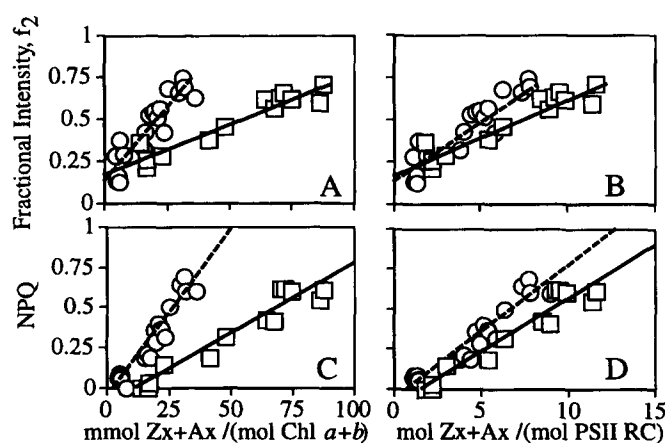


Figure 3. The relationship between the concentration of zeaxanthin and antheraxanthin [Zx+Ax] and both nonphotochemical quenching (NPQ) and the Lorentzian fractional intensity parameter f_2 in barley wild-type (circles) and *chlorina* f104 (squares) thylakoids. The Zx+Ax concentration is expressed relative to both Chl *a+b* (A,C) and the estimated number of PS II reaction centers (B,D). The linear regression statistics are given in Table 2. The xanthophyll cycle pool sizes for the WT and f104 thylakoids were 68.0 ± 0.7 and $120.0 \pm 3.0 \mu\text{mol} [Vx+Zx+Ax] (\text{mol Chl } a+b)^{-1}$, respectively.

na f104 were brought to within 65% (for f_2) and 80% (for NPQ) of those seen in the wild-type. Thus, we suggest that perhaps it is the concentration and, thus, binding frequency of these xanthophylls within the PS II inner antenna (independent of the peripheral antenna size) that determines the fraction of the Lorentzian f_2 component and thus NPQ in the presence of a constant

ΔpH . We further consider that the mol Zx+Ax/mol PS II ratio probably only roughly estimates the true effective concentration of Zx+Ax within the PS II inner antenna given that other factors, such as the levels of apoproteins of the Chl *b* containing light-harvesting complexes (Harrison et al. 1993; Preiss and Thornber

Table 3. Comparison of the mean \pm SE ratios^a of the PS II Chl *a* fluorescence average lifetime values and intensity parameters under conditions of maximal and minimal rates of PS II photochemistry

Growth condition	Leaf sample	$\langle\tau\rangle_{F_m}/\langle\tau\rangle_{F_0}$	Steady state F_m/F_0	Steady state F_v/F_m
(Growth chamber) ^b	WT	5.89 ± 0.08	5.26 ± 0.12	0.809 ± 0.004
" "	<i>Chlorina</i> f104	6.99 ± 0.23	6.79 ± 0.08	0.851 ± 0.002
(Glasshouse)	WT $N_{pig} = 250^c$	5.20 ± 0.30	5.29 ± 0.10	0.810 ± 0.003
" "	<i>Chlorina</i> f2 $N_{pig} = 50$	4.04 ± 0.10	4.22 ± 0.15	0.761 ± 0.006

^aThe different growing conditions were described in the 'Materials and methods'.

^bThe values given are the pooled average for all three growth-chamber PFD conditions described in the 'Materials and methods'.

^c N_{pig} for the glasshouse grown WT and *chlorina* f2 barley was estimated based on data from Harrison et al. (1993), Knoetzel and Simpson (1991) and Bassi et al. (1993).

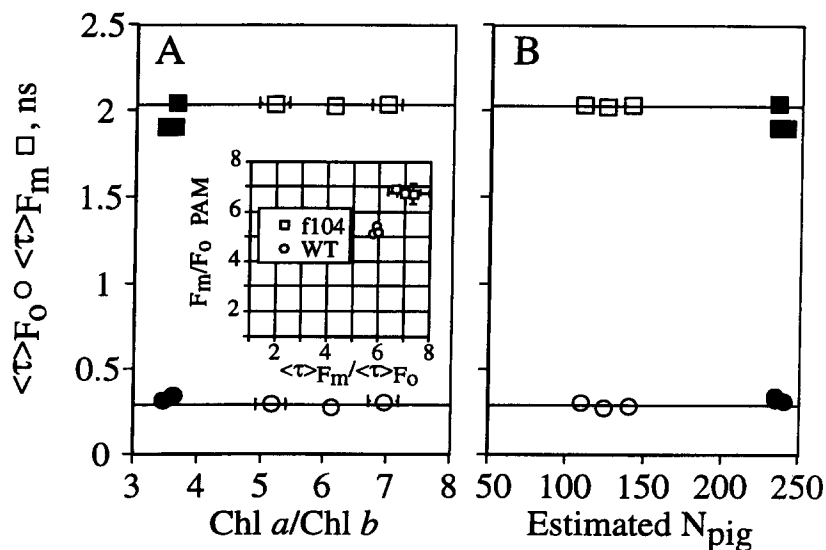


Figure 4. Relationships between (A) the Chl *a*/Chl *b* ratio and (B) the estimated PS II Chl *a*+*b* antenna size = N_{pig} and the average lifetimes of PS II Chl *a* fluorescence under conditions of maximal ($\langle\tau\rangle_{F_0}$) and minimal ($\langle\tau\rangle_{F_m}$) rates of photochemistry in barley wild-type and *chlorina* f104 leaves. The values shown in panel A are the Mean \pm SD for three parallel measurements for each ($\langle\tau\rangle_{F_0}$ and $\langle\tau\rangle_{F_m}$) versus Chl *a*/Chl *b* value; when not visible, the standard error bars were smaller than the symbol size. The average lifetime values $\langle\tau\rangle_{F_m}$ and $\langle\tau\rangle_{F_0}$ = $\sum f_x c_x$ were calculated using a three component and a two component exponential decay model, respectively. The inset in panel A shows the relationship between the ratio of $\langle\tau\rangle_{F_0}/\langle\tau\rangle_{F_m}$ and the ratio (F_m/F_0) of the PS II Chl *a* fluorescence intensity yields under conditions of maximal (F_0) and minimal (F_m) PS II photochemistry; the values shown are the Mean \pm SD of three parallel measurements for each of the three different growth chamber PFD conditions described in the 'Materials and methods'. The N_{pig} values in panel B were estimated based on the data presented by Knoetzel and Simpson (1991) and from the Chl *a*/Chl *b* ratios given in panel A.

1995), may affect the distribution and binding of the xanthophyll cycle pigments in the *chlorina* mutants.

The relationship between the PS II Chl a+b antenna size and the Chl a fluorescence lifetimes under conditions of maximal or minimal PS II photochemistry

In Figure 4 we compare the relationships between the Chl *a*/Chl *b* ratio (A), the estimated PS II Chl *a*+*b*

antenna size (B) and the average PS II Chl *a* fluorescence lifetimes under conditions of minimal and maximal PS II photochemistry, $\langle\tau\rangle_{F_m}$ and $\langle\tau\rangle_{F_0}$, respectively, in barley wild-type (filled symbols) and *chlorina* f104 leaves (open symbols). Figure 4A shows that the PS II Chl *a* fluorescence lifetimes remained constant when varying the Chl *a*/Chl *b* ratio by a factor of more than 2. The inset in Figure 2A shows that the ratio of the fluorescence intensity yields measured by the PAM under conditions of minimal and maximal

PS II photochemistry (F_m/F_o) correlated with the ratios of the average fluorescence lifetimes ($\langle\tau\rangle_{F_m}/\langle\tau\rangle_{F_o}$) under the same conditions. As reported by Knoetzel and Simpson (1991), the *chlorina* f104 leaves had significantly higher ratios than the wild-type leaves; this was apparently due to a combination of both slightly lower F_o and higher F_m yields. More importantly, the differences between the wild-type and *chlorina* f104 fluorescence yields were constant factors that were completely independent of the Chl *a*/Chl *b* ratio over the observed range. In the same manner, Figure 4B shows that both $\langle\tau\rangle_{F_m}$ and $\langle\tau\rangle_{F_o}$ remained constant when the estimated PS II Chl *a+b* antenna size (N_{pig}) varied from around 100 to almost 250.

In Table 3, we compare the $\langle\tau\rangle_{F_m}/\langle\tau\rangle_{F_o}$ ratios to the F_m/F_o and F_v/F_m ratios measured in parallel. As suggested in Figure 4, we show in Table 3 that the pooled average ratios for the growth chamber grown wild-type and *chlorina* f104 plants were constant and, therefore, independent of the growth PFD. The ratios were significantly higher for the *chlorina* f104 leaves than for the wild-type leaves. The glasshouse grown barley *chlorina* f2 leaves had Chl *a*/Chl *b* ratios approaching infinity and estimated N_{pig} values of around 50 mols of Chl *a* per PS II. Their F_m/F_o and $\langle\tau\rangle_{F_m}/\langle\tau\rangle_{F_o}$ ratios were both around 4, i.e., significantly lower than the wild-type (≥ 5). We found the lowered ratios were mostly due to a lower $\langle\tau\rangle_{F_m} = 1.89 \pm 0.03$ ns in the *chlorina* f2 leaves than the wild type leaves where $\langle\tau\rangle_{F_m} = 2.12 \pm 0.02$ ns; indeed, the $\langle\tau\rangle_{F_o} \approx 400$ ps values were very similar, being only slightly higher for the *chlorina* f2 than the wild-type leaves. Consistent with our results, Briantais et al. (1996), using the single-photon counting method to analyze the flash decay, observed that the average PS II Chl *a* fluorescence lifetimes at F_o were virtually identical for wild-type and *chlorina* f2 barley leaves. However, the average fluorescence lifetimes and intensity parameters from our work on both thylakoids and leaves were significantly higher than those obtained earlier with thylakoids by Searle et al. (1979) and Karukstis and Sauer (1984). In all likelihood, the decreased fluorescence lifetimes and PS II photochemical efficiencies observed by these authors in isolated *chlorina* f2 thylakoids were due to thylakoid 'un-stacking', a problem that was thoroughly characterized by Bassi et al. (1985); reportedly only with very high Mg^{2+} (50 mM) and EDTA washing can isolated *chlorina* f2 thylakoids with depleted LHCIIB content be 're-stacked'. Under our experimental conditions, the

thylakoid unstacking was not a significant factor in the *chlorina* f104 thylakoids.

Discussion

As mentioned in the Introduction, the lifetimes of PS II Chl *a* fluorescence have been predicted to be proportional to the size of the antenna, i.e., the values of N_{pig} . This 'hypothesis' is quantitatively presented in Table 4 where we show calculations of the exciton lifetime (τ_{life}) based on representative N_{pig} values of the wild-type and *chlorina* mutant material from this study; the exciton lifetime (τ_{life}) should have been directly proportional to the measured fluorescence lifetime. Here for simplicity, we use a homogeneous, 2-dimensional square-lattice model of PS II antenna organization (Pearlstein 1982). Theoretically, τ_{life} is the sum of both the lifetime of the exciton diffusion process in the antenna (τ_{diff}) and the lifetime of the trapping process of the reaction center (τ_{trap}) (see Dau 1994). It is clear from the formulas of these parameters given in the legend of Table 4 that τ_{diff} and τ_{trap} would expectedly increase with increasing N_{pig} . Clearly, the expected 2 and 5 fold decreases in τ_{life} in *chlorina* f104 and f2, respectively, as compared to the WT were not observed in our experimentally obtained fluorescence lifetime data. Moreover, even when we consider that the PS II antenna organization is both spectrally and structurally heterogeneous, our data still do not fit the general assumption that the residence probability of the exciton on the P680 Chls or p680 is equal to $c_H N_{pig}^{-1}$, where the c_H term accounts for spectral heterogeneity in the PS II unit (see Dau 1994).

However, our findings regarding the antenna size independence of the average lifetime under F_m conditions corroborate Tyystjärvi et al. (1994). Their review of the literature showed that the average lifetime at F_m is independent of N_{pig} . They hypothesized that the lifetime of the exciton should only be governed by N_{pig} if the rate constant of charge separation in the reaction center is fast relative to the exciton diffusion throughout the antenna. According to their argument under F_o conditions, when the rate constant of charge separation is six times faster than at F_m (Schatz et al. 1988), the average lifetime may be proportional to N_{pig} . Thus, it also follows from their logic that if F_m remains constant and F_o decreases in proportion to N_{pig} , then $F_v = F_m - F_o$ might increase if the antenna size becomes smaller. However, to our knowledge most higher plants (Björkman and Demmig 1987) including those in this

Table 4. Predicted values for the PS II exciton lifetime (τ_{life}), which is the sum of the lifetime of diffusion of the exciton in the antenna (τ_{diff}) and the lifetime of exciton trapping by the reaction center (τ_{trap}), based on a homogeneous, 2-dimensional square lattice with the number of lattice sites equal to N_{pig} (Pearlstein 1982)

	$N_{\text{pig}}^{\text{a}}$	$\tau_{\text{diff}}^{\text{b}}$	$\tau_{\text{trap}}^{\text{c}}$	$\tau_{\text{life}} = \tau_{\text{diff}} + \tau_{\text{trap}}$
WT	250	488 ps	750 ps	1238 ps
<i>Chlorina</i> f104	133	233 ps	399 ps	632 ps
<i>Chlorina</i> f2	50	72 ps	150 ps	222 ps

^a N_{pig} values were estimated for the wild-type and *chlorina* f104 and f2 material from the data presented in Knoetzel and Simpson (1991).

^b $\tau_{\text{diff}} = N_{\text{pig}} c_{\text{geo}} k_{\text{T}}^{-1}$, where $c_{\text{geo}} = (0.318 \ln N_{\text{pig}} + 0.195)$ is the geometry factor for a 2-dimensional square lattice (Pearlstein 1982) and $k_{\text{T}}^{-1} = 1$ ps is the assumed lifetime for energy transfer between lattice sites.

^c $\tau_{\text{trap}} = N_{\text{pig}} k_1^{-1}$, where $k_1^{-1} = 3$ ps is the assumed average lifetime of PS II primary charge separation.

study (Table 3) and other studies on barley *chlorina* mutants (Briantais 1994; Falk et al. 1994a,b; Lokstein et al. 1994) show similar F_v/F_m ratios generally ranging around 0.75 to 0.85. Also, directly pertinent to any proposed relationship between N_{pig} and F_v/F_m there is apparently no correlation between the PS II antenna size and the constant F_v/F_m ratio in either greening plants (Björkman and Demmig 1987; Briantais 1994) or senescing plants (Adams et al. 1990b) or when comparing leaves from barley wild-type and *chlorina* f2 and f104 mutants (Briantais 1994). Thus, based on the present literature and our data, no direct relationship between N_{pig} and the fluorescence lifetimes or yields at F_0 , F_m or F_v/F_m is supported.

We further consider the implications of the antenna size independent relationships of our data in relation to the exciton radical pair equilibrium model of Holzwarth and co-workers (Schatz et al. 1988; Holzwarth 1988). This model assumes that the entire PS II unit (LHC+CORE+P680) behaves as a single pigment pool, where the exciton rapidly equilibrates among all the Chls including P680. Therefore, in the exciton radical pair model it is assumed that any changes in the fluorescence lifetimes under F_0 conditions must be due to either 1) changes in the number of Chl molecules in the PS II antenna, 2) changes that affect energy transfer rates among the PS II antenna and reaction center Chls (including molecular orientation, spacing, pigment-protein complex conformation etc.) or 3) changes that affect the reaction center structure and photochemistry (and thus either k_1 = rate constant of charge separation, k_{-1} = rate constant of charge recombination or k_2 = rate constant of charge

stabilization). As shown in this paper, and as discussed above, there are no significant differences between the WT and *chlorina* mutant fluorescence lifetimes which suggests that there are no major (2 to 5 fold) differences in PS II reaction center photochemistry under F_0 conditions. Further, our data show that the relationship between the PS II Chl *a* fluorescence lifetimes and intensity under xanthophyll cycle-dependent NPQ conditions are virtually identical between the wild-type and *chlorina* f104 mutant (Table 1, Figure 2). Because the xanthophyll cycle effects are apparently occurring in the antenna, our data strongly suggest that the energy transfer processes of the PS II antenna basically remain unchanged between the *chlorina* f104 mutant and the wild-type. Therefore, we consider it unlikely that either changes in the photochemical rate constants in the reaction center and/or the energy transfer processes in the antenna systematically compensate for the N_{pig} differences between the *chlorina* and wild-type materials to result in the similar fluorescence lifetimes.

In essence, our data suggest that the exciton lifetime, as determined by the probability of deexcitation by either photochemical charge separation, charge stabilization or heat dissipation (NPQ), is not affected by changes in the N_{pig} . However, it is well known that increases in the PS II antenna size increase the absorbance cross section and the probability that the PS II unit will absorb a photon for any given PFD. The decreased absorbance cross section of the *chlorina* PS II units, compared to those of the wild-type, correlate directly with a decreased rate (or increased $t_{1/2}$) for fluorescence induction from F_0 to F_m (Q_A reduction) in the *chlorina* mutants (Knoetzel and Simpson 1991; Leverenz et al 1992; Falk et al. 1994a). Thus, the quantum yield for the overall rate of PS II photochemistry (measured as Q_A reduction) is, obviously, lower in the *chlorina* mutants than in the wild-type barley. However, the fluorescence lifetime values at F_m and F_0 and, thus, the F_v/F_m ratio remain relatively constant independent of the absorption cross section or the number of photons absorbed by the PS II unit per unit time.

One hypothesis to explain how the PS II fluorescence lifetimes remain constant independent of the N_{pig} is to propose that the peripheral antenna (mainly LHCI-Ib) efficiently transfers all excitation to the PS II core and inner antenna which then fluoresces; LHCI-Ib *in vivo* is thus expected to have very low or no fluorescence due to a high rate constant of energy transfer. This suggestion is consistent with established literature that shows that there is normally little or no fluorescence (i.e., fluorescence at 680 nm, F680) from LHCI-Ib

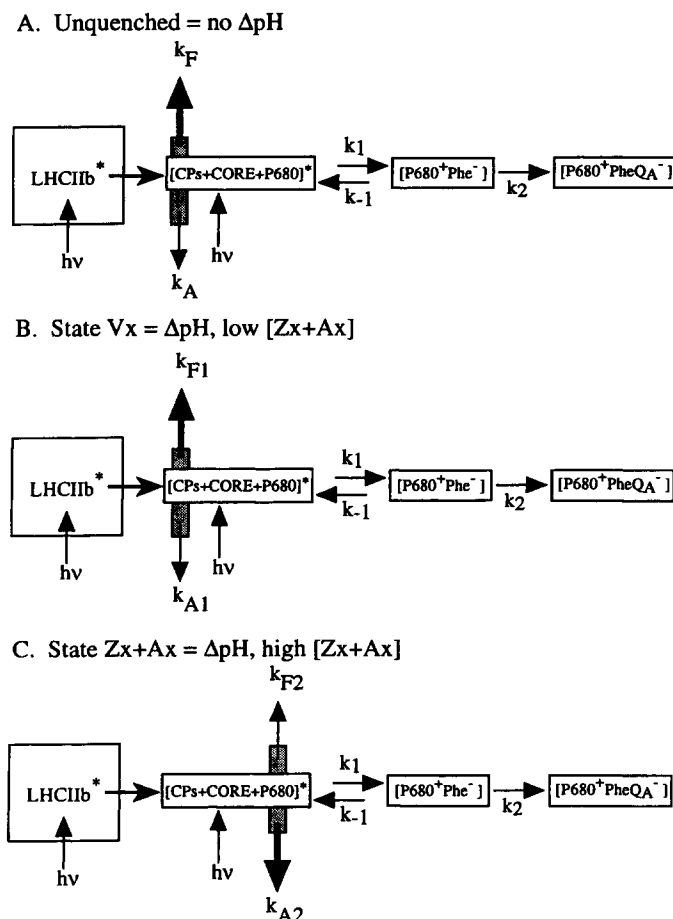


Figure 5. A scheme for the gross structure and function of PS II to explain both the role of the peripheral PS II antenna (LHCIIb) and the xanthophyll cycle-dependent NPQ mechanism. We assume here that no fluorescence appears from the peripheral antenna (LHCIIb) because there is an extremely efficient energy transfer from LHCIIb to the PS II core plus inner antenna. Here we also assume that rapid exciton equilibration occurs only in the PS II core plus inner antenna (here defined to include D1, D2, all CP proteins (24, 26, 29, 43, 47) and P680). The rate constants are defined as: k_F for fluorescence, k_1 for charge separation, k_{-1} for charge recombination, k_2 for charge stabilization and k_A for all combined energy dissipation pathways in the PS II antenna except photochemistry and fluorescence. Panel A shows the conditions without a ΔpH , thus, there is no fluorescence quenching (i.e., unquenched conditions). In Panel B, for state V_x , there is a ΔpH and the new rate constant k_{A1} and corresponding k_{F1} are proposed because the fluorescence lifetime center (c_1) and width (w_1) parameters differ significantly from those in the absence of a ΔpH (Panel A). In Panel C, for state $Z_x + A_x$, there is a ΔpH and the rate constant k_{A2} determines the increased heat dissipation in the PS II unit.

as observed *in vivo*. F680 can be seen if 1) the thylakoid material is treated with detergent to disrupt the energy transfer link between LHCIIb and the fluorescent PS II core, or, 2) the temperature is lowered to 4K (see review by Briantais et al. 1986). It can be seen at temperatures as high as 110K in intact spinach chloroplasts (Knox and Lin 1988) and *Chlamydomonas reinhardtii* cells (Lin and Knox 1991) by deconvolution of streak-camera data, which confirm that it has a very short lifetime because of transfer. It is absent in the barley *chlorina* f2 mutants (Rijgersberg et al. 1979; Krugh and

Miles 1995), and in *Chlamydomonas* mutants lacking LHC or lacking PS-II (Lin and Knox 1991).

Regarding the relationship between N_{pig} and xanthophyll cycle-dependent NPQ, it is clear from our data (Figure 3, Table 2) and earlier studies (Falbel et al. 1994; Lokstein et al. 1994) that the increased ratio of $[Z_x + A_x] : [Chl\ a + b]$ in the *chlorina* mutants does not increase the level of NPQ over that seen in the wild-type. We therefore conclude that the level of NPQ is not determined simply by the ratio of $[Z_x + A_x] : [Chl\ a + b]$. To explain this, we suggest that the extent of NPQ in the presence of a ΔpH is deter-

mined by the binding of the Zx+Ax molecules to the protonated CP complexes of the PS II inner antenna; thus, NPQ is mostly independent of the levels of LHCIb in the peripheral antenna within the ranges of N_{pig} examined in this paper. This idea could explain how the decreased levels of the inner antenna CP proteins in the Chl *b*-less *chlorina* mutants (Harrison et al. 1993, Preiss and Thornber 1995) could decrease the capacity for NPQ (Falk et al. 1994b; Lokstein et al. 1994; Härtel and Lokstein 1995) by decreasing the number of xanthophyll binding sites per PS II unit. Clearly the lower levels of Chl *b* (LHCIb) in the *chlorina* f104 mutant, compared to the wild-type, do not inhibit the final levels of Vx deepoxidation, the fluorescence lifetimes or NPQ under our conditions. Importantly, according to Knoetzel and Simpson (1991), the high-light grown *chlorina* f104 retains near wild-type levels of all the minor CP complexes and becomes deficient in only two mature Chl *b* containing complexes, namely LHCIb and LHCI680. As mentioned before, Bassi et al. (1993) reported that the majority of the xanthophyll cycle pigments ($\approx 80\%$) are concentrated in these minor CP complexes. Jahns and Schweig (1995) reported that the xanthophyll-NPQ function probably involves the CP26 protein because this is the only Chl *a/b* protein expressed in intermittent light grown pea plants that have significant levels of xanthophyll cycle-dependent NPQ. We therefore conclude that the similarities in the level of Vx deepoxidation (and Zx+Ax/PS II ratio) between the *chlorina* f104 and wild-type thylakoids are consistent with the Zx+Ax-CP binding hypothesis. Further, our observations suggest that binding of Zx+Ax by LHCIb does not play a major role in NPQ. It is also important to consider that perhaps the presence or binding of Zx+Ax within LHCIb or the apoproteins of the Chl *b* containing complexes may not influence the absolute concentrations of Zx+Ax in the PS II inner antenna.

We summarize in Figure 5 an interpretation of the fluorescence lifetime results in this study first with respect to the role of the peripheral PS II antenna (LHCIb) and then with respect to the xanthophyll cycle-dependent NPQ mechanism. We propose, as already mentioned earlier, that the peripheral light-harvesting antenna (mostly LHCIb) transfers energy with high efficiency to the PS II reaction center core plus inner antenna (see Figure 5 legend). Because it is a highly efficient energy transfer there is no fluorescence from LHCIb at room temperature. Although our model implies that the peripheral and inner antenna may not be in excitonic equilibrium, we retain the hypothesis

that there is a rapid exciton equilibration within the PS II core plus inner antenna, i.e., similar to Schatz et al. (1988). However, we suggest that further experiments are needed to determine the effects of changes in the number of Chls within the PS II core plus inner antenna on the PS II Chl *a* fluorescence lifetimes. The most important result of this paper is that whether the PS II core plus inner antenna units are excited directly by light absorption (as in the *chlorina* mutants, with depleted peripheral antennae) or indirectly by energy transfer from the peripheral antenna (wild-type) the PS II Chl *a* fluorescence lifetimes are the same.

Regarding the xanthophyll cycle-dependent NPQ mechanism, Figure 5 shows that for all PS II units, the rate constant k_A comprises all energy dissipation processes including internal conversions from the antenna except photochemistry or fluorescence. In the absence of a ΔpH (Figure 5A, unquenched), the xanthophyll cycle pigments Zx and Ax are not engaged in quenching of the Chl fluorescence because the CP proteins are not protonated. The main lifetime distribution, c_1 , under the unquenched conditions is explained by the fact that all the unprotonated PS II units have similar overall structural conformations and thus similar fluorescence lifetimes. However, when there is a ΔpH and CP-protonation, the PS II units are either in state Vx (Figure 5B) or state Zx+Ax (Figure 5C); the rate constants k_{A1} (state Vx) or k_{A2} (state Zx+Ax), respectively, determine the dissipation of energy in the antenna other than that not due to reaction center photochemistry or fluorescence. The PS II units in state Vx have a fraction of their xanthophyll binding proteins protonated and activated for potential binding, and the ΔpH -dependent conformational changes are suggested to cause the narrowing and shortening of the c_1 lifetime distribution (Figure 1, Table 1). The fraction of PS II units in state Zx+Ax depends on the [Zx+Ax]; PS II units in state Zx+Ax are suggested to be the source of the c_2 distribution under the quenched condition (Gilmore et al. 1995a,b). We suggest that an increase in the heat loss portion of the antenna dissipation rate constant (k_{A2}) decreases the fluorescence lifetime ($\propto 1/k_{F2}$). We here envision a situation where the xanthophylls Zx+Ax bind (and quench) with a frequency per PS II unit that is proportional to the [Zx+Ax]. We deduced from experiments with the zeaxanthin epoxidation reaction, that reverses NPQ in the presence of a ΔpH (Gilmore et al. 1994), that the putative NPQ binding sites must bind and release Zx and Ax with a certain frequency, thus, helping to explain our 2-state PS II model for xanthophyll cycle-dependent NPQ.

Interestingly, our 2-state PS II model of NPQ is similar in some aspects to the model proposed earlier by Weis and Berry (1987). The final quenched complex (state $Zx+Ax$) is possibly due to a major conformational switch, mediated by the pH-dependent binding of the deepoxidized endgroups of Zx or Ax to the CP complexes, that causes a very strong heat dissipation within the PS II unit. Importantly, like the exciton radical pair equilibrium model of Schatz et al. (1988) from which our picture was derived, the model in Figure 5 predicts that increasing the rate constant of heat dissipation (k_{A2}) should quench the F_o fluorescence level in linear proportion to the F_m level; indeed, this has been clearly shown in thylakoid systems similar to those used in this study (Gilmore and Yamamoto 1992; Gilmore et al. 1995a,b).

Regarding the concerted effects of both the ΔpH and $[Zx+Ax]$ on the NPQ mechanism, one must consider that when proton-pumping by both light-saturated electron transport and the ATPase are combined for a given $[Zx+Ax]$, the ΔpH and thus NPQ are both larger than with H^+ pumping by only the ATPase (see Figure 2). Thus, based on the above arguments we predict that increasing the lumen $[H^+]$ in the light would increase the fraction of protonated CP complexes (binding sites for $Zx+Ax$ per PS II unit) and increase the fraction of PS II units in state $Zx+Ax$ at any given time and for any given $[Zx+Ax]$. Interestingly, it seems that the largest differences in the ratios of the V_x and $Zx+Ax$ states (f_1 and f_2 fractional intensities) in barley thylakoids occurs in the range of NPQ below 1. According to our estimations in Figure 2, the ratio of NPQ to f_2 should increase more steeply then saturate as the fraction of the f_2 component approaches a value of 1.

Our time-resolved data and conclusions about the site of NPQ in the inner PS II antenna have important implications with respect to the functioning of the NPQ mechanism under conditions of extremely high ΔpH and low concentrations of $Zx+Ax$. Because we estimated that the dark-adapted levels of $Zx+Ax$ are around 2 mols per mol PS II in barley leaves and thylakoids (Figure 3) it is possible that in the presence of a very high ΔpH these background levels of $Zx+Ax$ may lead to substantial levels of NPQ. Indeed, the highest levels of deepoxidation (Figure 3) did not increase the ratio of $Zx+Ax/PS II$ by much more than a factor of five or six over the dark adapted levels (Figure 3). Here we also speculate that increasing the ΔpH may decrease the fluorescence lifetime center of c_1 (in the quenched state) even further than documented in Figure 1 and Table 1. Thus, we propose that the combination of

a ΔpH -dependent decrease in the lifetime center of the main lifetime distribution and the conversion to state $Zx+Ax$ with a high ΔpH and only low $[Zx+Ax]$ could result in NPQ that is 'apparently' independent of the xanthophyll cycle mechanism. We propose that these factors could possibly explain a substantial portion of 'xanthophyll cycle-independent' quenching of fluorescence in high-light-adapted leaves, that have a high ΔpH but only low levels of $Zx+Ax$ (Adams et al. 1990a; Bilger and Björkman 1991). Indeed, these possibilities were discussed in an earlier study by Gilmore and Yamamoto (1993) where it was shown that both the ΔpH and $[Zx+Ax]$ may have separate as well as concerted effects on the PS II Chl *a* fluorescence intensity.

Acknowledgements

AMG was supported by a training grant (DOE 92ER20095) from the Triagency (DOE/NSF/USDA) Program for Collaborative Research in Plant Biology (PGD and G are two of the several Co-PIs on this grant). TLH thanks NIH grant #RR03155. We thank Drs Barbara Demmig-Adams and William Adams III, their laboratory staff and graduate students for the use of their HPLC equipment and for stimulating discussions. We also thank Dr D. Simpson for the barley seeds and Ms Purna K. Lakhia for help in growing the barley and other laboratory assistance.

Note added in proof (April 17, 1996)

Dau and Sauer (1996) have recently presented a three compartment model describing the Photosystem II exciton dynamics consisting of a peripheral pigment pool (enriched in Chl *b*), an inner pigment pool of core PS II pigments and the primary radical pair compartment. We note that their model is similar in many aspects to ours (Figure 5) and it seems logical to assume that their peripheral pigment pool is the LHClIb compartment in our scheme.

References

- Adams WW III, Demmig-Adams B and Winter K (1990a) Relative contributions of zeaxanthin-related and zeaxanthin unrelated types of 'high-energy-state' quenching of chlorophyll fluorescence in spinach leaves exposed to various environmental conditions. *Plant Physiol* 92: 302-309
- Adams WW III, Demmig-Adams B, Winter K and Schreiber U (1990b) The ratio of variable to maximum fluorescence from Photosystem II, measured in leaves at ambient temperature and

- at 77K, as an indicator of the photon yield of photosynthesis. *Planta* 180: 166–174
- Andrews JR, Fryer MJ and Baker NR (1995) Consequences of LHCII deficiency for photosynthetic regulation in *chlorina* mutants of barley. *Photosynth Res* 44: 81–91
- Bassi R, Hinz U and Barbato R (1985) The role of light harvesting complex and Photosystem II in thylakoid stacking in the *chlorina-f2* barley mutant. *Carlsberg Res Commun* 50: 347–367
- Bassi R, Pineau B, Dainese P and Marquardt J (1993) Carotenoid-binding proteins of Photosystem II. *Eur J Biochem* 212: 297–303
- Bilger W and Björkman O (1991) Temperature dependence of violaxanthin de-epoxidation and non-photochemical fluorescence quenching in intact leaves of *Gossypium hirsutum* L. and *Malva parviflora* L. *Planta* 184: 226–234
- Björkman O and Demmig B (1987) Photon yield of O₂ evolution and chlorophyll fluorescence characteristics at 77K among vascular plants of diverse origins. *Planta* 170: 489–504
- Briantais J-M (1994) Light-harvesting chlorophyll *a-b* complex requirement for regulation of Photosystem II photochemistry by non-photochemical quenching. *Photosynth Res* 40: 287–294
- Briantais J-M, Verotte C, Krause GH and Weis E (1986) Chlorophyll *a* fluorescence of higher plants: Chloroplasts and Leaves. In: Govindjee, Amesz J and Fork DC (eds) *Light Emission by Plants and Bacteria*, pp 539–586. Academic Publishers, Orlando, FL
- Briantais J-M, Dacosta, J, Goulas Y, Ducruet J-M and Moya I (1996) Heat stress induces in leaves an increase of the minimum level of chlorophyll fluorescence. Fo. A time-resolved analysis. *Photosynth Res* 48: 189–196 (this issue)
- Butler W and Strasser RJ (1977) Tripartite model for the photochemical apparatus of green plant photosynthesis. *Proc Nat Acad Sci USA* 74: 3382–3385
- Crofts AR and Yerkes CT (1994) A molecular mechanism for quenching. *FEBS Lett* 352: 265–270
- Dau H (1994) Molecular mechanisms and quantitative models of variable Photosystem II fluorescence. *Photochem Photobiol* 60: 1–23
- Dau H and Sauer K (1996) Exciton equilibration and Photosystem II exciton dynamics – a fluorescence study on Photosystem II membrane particles of spinach. *Biochim Biophys Acta* 1273: 175–190
- Demmig-Adams B, Gilmore AM and Adams WW III (1996) *In vivo* functions of carotenoids in higher plants. *FASEB* 10: 203–214
- Emerson R and Arnold A (1932a) A separation of the reactions in photosynthesis by means of intermittent light. *J Gen Physiol* 15: 391–420
- Emerson R and Arnold A (1932b) The photochemical reaction in photosynthesis. *J Gen Physiol* 16: 191–205
- Falbel TG, Staehelin A and Adams WW III (1994) Analysis of xanthophyll cycle carotenoids and chlorophyll fluorescence in light intensity-dependent chlorophyll-deficient mutants of wheat and barley. *Photosynth Res* 42: 191–202
- Falk S, Bruce D and Huner NPA (1994a) Photosynthetic performance and fluorescence in relation to antenna size and absorption cross-sections in rye and barley grown under normal and intermittent light conditions. *Photosynth Res* 42: 145–155
- Falk S, Król M, Maxwell DP, Rezansoff DA, Gray GR and Huner NPA. (1994b) Changes in the *in vivo* fluorescence quenching in rye and barley as a function of reduced PS II light-harvesting antenna size. *Physiol Plant* 91: 551–558
- Frauenfelder H, Parak F and Young RD (1988) Conformational substates in proteins. *Ann Rev Biophys Biophys Chem* 17: 451–479
- Gaffron H and Wohl K (1936) Zur Theorie der Assimilation. *Naturwissenschaften* 24: 81–90, 103–107
- Gilmore AM and Björkman O (1995) Temperature-sensitive coupling and uncoupling of ATPase-mediated, nonradiative energy dissipation: Similarities between chloroplasts and leaves. *Planta* 197: 646–654
- Gilmore AM and Yamamoto HY (1991) Resolution of lutein and zeaxanthin using a nonendcapped, lightly carbon-loaded C-18 high-performance liquid chromatographic column. *J Chromatogr* 543: 137–145
- Gilmore AM and Yamamoto HY (1992) Dark induction of zeaxanthin-dependent nonphotochemical fluorescence quenching mediated by ATP. *Proc Natl Acad Sci USA* 89: 1899–1903
- Gilmore AM and Yamamoto HY (1993) Linear models relating xanthophylls and lumen acidity to non-photochemical fluorescence quenching. Evidence that antheraxanthin explains zeaxanthin-independent quenching. *Photosynth Res* 35: 67–78
- Gilmore AM, Hazlett TL and Govindjee (1995a) Xanthophyll cycle dependent quenching of Photosystem II chlorophyll *a* fluorescence: formation of a quenching complex with a short fluorescence lifetime. *Proc Natl Acad Sci USA* 92: 2273–2277
- Gilmore AM, Hazlett TL, Björkman O and Govindjee (1995b) Xanthophyll cycle dependent non-photochemical quenching of chlorophyll *a* fluorescence at low physiological temperatures. In: Mathis P (ed) *Photosynthesis: From Light to Biosphere*, Vol IV, pp 825–828. Kluwer Academic Publishers, Dordrecht, The Netherlands
- Govindjee (1995) Sixty-three years since Kautsky: Chlorophyll *a* fluorescence. *Aust J Plant Physiol* 22: 131–160
- Govindjee, Van de Ven M, Cao J, Royer C and Gratton E. (1993) Multifrequency cross-correlation phase fluorometry of chlorophyll *a* fluorescence in thylakoid and PS II-enriched membranes. *Photochem Photobiol* 58: 438–445
- Graan T and Ort DR (1984) Quantitation of the rapid electron donors to P700, the functional plastoquinone pool, and the ratio of the photosystems in spinach chloroplasts. *J Biol Chem* 259: 14003–14010
- Hager A (1969) Lichtbedingte pH-Erniedrigung in einem Chloroplasten-Kompartiment als Ursache der enzymatischen Violaxanthin→Zeaxanthin-Umwandlung; Beziehungen zur Photophosphorylierung. *Planta* 89: 224–243
- Harrison MA, Nemson JA and Melis A (1993) Assembly and composition of the chlorophyll *a-b* light-harvesting complex of barley (*Hordeum vulgare* L.): Immunochemical analysis of chlorophyll *b*-less and chlorophyll *b*-deficient mutants. *Photosynth Res* 38: 141–151
- Härtel H and Lokstein H (1995) Relationship between quenching of maximum and dark-level chlorophyll fluorescence in vivo: dependence on Photosystem II antenna size. *Biochim Biophys Acta* 1228: 91–94
- Holzwarth AR (1988) Time resolved chlorophyll fluorescence. What kind of information does it provide? In: Lichtenthaler HK (ed) *Applications of Chlorophyll Fluorescence in Photosynthesis, Stress Physiology, Hydrobiology and Remote Sensing*, pp 21–31. Kluwer Academic Publishers, Dordrecht, The Netherlands
- Horton P, Ruban AV and Walters RG (1994) Regulation of light harvesting in green plants. *Plant Physiol* 106: 415–420
- Jahns P and Schweig S (1995) Energy-dependent fluorescence quenching in thylakoids from intermittent light grown pea plants – evidence for an interaction of zeaxanthin and the chlorophyll *a/b* binding protein CP26. *Plant Physiol Biochem* 33: 683–687
- Karukstis KK and Sauer K (1984) Organization of the photosynthetic apparatus of the *chlorina-f2* mutant of barley using chlorophyll fluorescence decay kinetics. *Biochim Biophys Acta* 766: 148–155

- Knoetzel J and Simpson D (1991) Expression and organization of antenna proteins in the light- and temperature-sensitive barley mutant *chlorina*-104. *Planta* 185: 111–123
- Knox RS (1975) Excitation energy transfer and migration: Theoretical considerations. In: Govindjee (ed) *Bioenergetics of Photosynthesis*, pp 183–224. Academic Press, New York
- Knox RS and Lin S (1988). Time resolution and kinetics of 'F680' at low temperatures in spinach chloroplasts. In: Scheer H and Schneider S (eds) *Photosynthetic Light Harvesting Systems: Structure and Function*, pp 567–577. Walter de Gruyter, Berlin
- Krugh BW and Miles D (1995) Energy transfer for low temperature fluorescence in PS II mutant thylakoids. *Photosynth Res* 44: 117–125
- Leverenz JW, Öquist G and Wingsle G (1992) Photosynthesis and photoinhibition in leaves of chlorophyll *b*-less barley in relation to absorbed light. *Physiol Plant* 85: 495–502
- Lin S and Knox RS (1991) Studies of excitation energy transfer within the green alga *Chlamydomonas reinhardtii* and its mutants at 77K. *Photosynth Res* 27:157–168
- Lokstein H, Härtel H, Hoffman P, Woitke P and Renger G (1994) The role of light-harvesting complex II in excess excitation energy dissipation: An *in-vivo* fluorescence study on the origin of high-energy quenching. *Photochem Photobiol* 26: 175–184
- Mills JD and Mitchell P (1982) Modulation of coupling factor ATPase activity in intact chloroplasts. Reversal of thiol modulation in the dark. *Biochim Biophys Acta* 679: 75–83
- Pearlstein RM (1982) Chlorophyll singlet excitons. In: Govindjee (ed) *Photosynthesis: Energy Conversion by Plants and Bacteria*, pp 294–391. Academic Press, New York
- Petrack B and Lipman, F. (1961) Photophosphorylation and photohydrolysis in cell-free preparations of blue-green algae. In: McElroy WD and Glass B (eds) *Light and Life*, pp 621–630. Johns Hopkins Press, Baltimore, MD
- Porra RJ, Thompson WA and Kriedmann PE (1989) Determination of accurate extinction coefficients and simultaneous equations for assaying chlorophylls *a* and *b* extracted with four different solvents: Verification of the concentration of chlorophyll standards by atomic absorption spectroscopy. *Biochim Biophys Acta* 975: 384–394
- Preiss S and Thornber JP (1995) Stability of the apoproteins of light-harvesting complex I and II during biogenesis of thylakoids in the chlorophyll *b*-less barley mutant *chlorina f-2*. *Plant Physiol* 107: 709–717
- Rijgersberg CP, Ames J, Thielen APGM and Swager JA (1979) Fluorescence emission spectra of chloroplasts and subchloroplast preparations at low temperatures. *Biochim Biophys Acta* 545: 473–482
- Schatz GH, Brock H and Holzwarth AR (1988) A kinetic and energetic model for the primary processes in Photosystem II. *Biophys J* 54: 397–405
- Searle GFW, Tredwell CJ, Barber J and Porter G (1979) Picosecond time-resolved study of chlorophyll organization and excitation energy distribution in chloroplasts from wild-type barley and a mutant lacking chlorophyll *b*. *Biochim Biophys Acta* 545: 496–507
- Simpson D, Machold O, Høyer-Hansen G and von Wettstein D (1985) *Chlorina* mutants of barley (*Hordeum vulgare* L.). *Carlsberg Res Commun* 50: 223–238
- Tyystjärvi E, Kettunen R and Aro E-M (1994) The rate constant of photoinhibition *in vitro* is independent of the antenna size of Photosystem II but depends on temperature. *Biochim Biophys Acta* 1186: 177–185
- van Grondelle R, Dekker JP, Gillbro T and Sundstrom V (1994) Energy transfer and trapping in photosynthesis. *Biochim Biophys Acta* 1187: 1–65
- van Kooten O and Snel JFH (1990) The use of chlorophyll fluorescence nomenclature in plant stress physiology. *Photosynth Res* 25: 147–150
- Visser HM, Somsen OJG, van Mourik F, Lin S, van Stokkum IHM and van Grondelle R (1995) Direct observation of sub-picosecond equilibration of excitation energy in the light-harvesting antenna of *Rhodospirillum rubrum*. *Biophys J* 69: 1083–1099
- Walters RG, Ruban AV and Horton P (1994) Higher plant light-harvesting complexes LHCIIa and LHCIIc are bound by dicyclohexylcarbodiimide during inhibition of energy dissipation. *Eur J Biochem* 226: 1063–1069
- Weis E and Berry JA (1987) Quantum efficiency of Photosystem II in relation to 'energy'-dependent quenching of chlorophyll fluorescence. *Biochim Biophys Acta* 894: 198–207
- Yamamoto HY and Bassi R (1996) Carotenoids: Localization and Function. In: Ort DR and Yocum CF (eds) *Oxygenic Photosynthesis: The Light Reactions*. *Advances in Photosynthesis*, Vol 4, pp 539–563. Kluwer Academic Publishers, Dordrecht, The Netherlands
- Yamamoto HY and Kamite L (1972) The effects of dithiothreitol on violaxanthin de-epoxidation and absorbance changes in the 500-nm region. *Biochim Biophys Acta* 267: 538–543
- Yamamoto HY, Nakayama TOM and Chichester CO (1962) Studies on the light and dark interconversions of leaf xanthophylls. *Arch Biochem Biophys* 97: 168–173